Impact of additional genetic abnormalities at diagnosis of chronic myeloid leukemia for first-line imatinib-treated patients receiving proactive treatment intervention

Naranie Shanmuganathan,[1,2,3,4,5,6,7] Carol Wadham,[2,3,5] NurHezrin Shahrin,[2,3] Jinghua Feng,[5,8] Daniel Thomson,[2,3] Paul Wang,[3,8] Verity Saunders,[4] Chung Hoow Kok,[4,5,6] Rob M. King,[8] Rosalie R. Kenyon,[8] Ming Lin,[8] Ilaria S. Pagani,[4,6,7] David M. Ross,[1,2,3,4,7,9] Agnes S.M. Yong,[4,6,7,10] Andrew P. Grigg,[7,11] Anthony K. Mills,[7,12] Anthony P. Schwarer,[7,13] Jodi Braley,[2] Haley Altamura,[2] David T. Yeung,[1,4,5,6,7] Hamish S. Scott,[2,3,5,6,8] Andreas W. Schreiber,[3,8,14] Timothy P. Hughes[1,4,6,7] and Susan Branford[2,3,4,5,6]

[1]Department of Hematology, Royal Adelaide Hospital and SA Pathology, Adelaide; [2]Department of Genetics and Molecular Pathology, SA Pathology, Adelaide; [3]Centre for Cancer Biology, SA Pathology and University of South Australia, Adelaide; [4]Precision Cancer Medicine Theme, South Australian Health & Medical Research Institute (SAHMRI), Adelaide; [5]Clinical and Health Sciences, University of South Australia, Adelaide; [6]Adelaide Medical School, University of Adelaide, Adelaide; [7]Australasian Leukemia and Lymphoma Group (ALLG); [8]Australian Cancer Research Foundation Genomics Facility, Centre for Cancer Biology, SA Pathology, Adelaide; [9]Department of Hematology, Flinders University and Medical Centre, Adelaide; [10]The University of Western Australia Medical School, Western Australia; [11]Department of Clinical Hematology, Austin Hospital and University of Melbourne, Melbourne; [12]Department of Hematology, Princess Alexandra Hospital, Brisbane; [13]Department of Hematology, Box Hill Hospital, Melbourne and [14]School of Biological Sciences, University of Adelaide, Adelaide, Australia

Correspondence: N. Shanmuganathan
naranie.shanmuganathan@sa.gov.au

Received: October 6, 2022.
Accepted: March 16, 2023.
Early view: March 23, 2023.

https://doi.org/10.3324/haematol.2022.282184

Supplement

Title: Impact of additional genetic abnormalities at diagnosis of chronic myeloid leukemia for first-line imatinib-treated patients receiving proactive treatment intervention

Supplemental methods

Medication compliance assessment

Patient compliance assessments were included in the CML9 (TIDEL-II) study protocol and are as follows.

- Imatinib trough levels were performed on day 22 of imatinib therapy and patients with trough levels <1,000ng/mL who were confirmed to be compliant with imatinib administration underwent dose escalation to a total daily dose of imatinib of 800mg.
- Records of dosing diaries, dosages administered and returned as well as the interval between study visits were recorded by study personnel.
- Imatinib and/or nilotinib drug accountability was logged by the pharmacy and study staff of each study centre.
- Patients with questionable study compliance were reported to the study management committee and patients deemed to be non-compliant were withdrawn from the study following discussion with the treating physician.

Next-generation sequencing

The genes selected for inclusion in the customized panel were either recurrently mutated in CML[1] or commonly reported in acute leukemias. Specific intronic regions of *BCR* were targeted by probes to detect the genomic breakpoints of the common e13a2 and e14a2 *BCR::ABL1* fusions. To maximise the detection of Ph-associated rearrangements, we included additional genes on chromosomes 9 and 22. Furthermore, probes targeted intronic cryptic *RAG* recombination signal sequences of specific genes for the detection of *RAG*-mediated deletions, including *IKZF1* (Supplemental Table 1). The STAR algorithm aligned the raw sequencing data to the hg19 reference genome.[2] Genomic breaks were detected using total RNA due to the presence of intron-retaining precursor mRNA, usually absent from standard poly(A) enriched RNA-seq.[3] The detection of Ph-associated rearrangements was possible, even if only one of the fusion partner regions was captured, through spanning reads that partially mapped to the partner gene. Some events were the product of deletion-bridges,[4] which were identified by copy number variation analysis or aberrant splicing.[5] Other Ph-associated rearrangements were derived from variant translocations, as evidenced by chromosome analysis.

Additional detail regarding sequencing and validation methods has been published elsewhere.[3, 5] The variant callers were VarDict[6] and Mutect2.[7] Strict criteria were used to assess the pathogenicity of each SNV and indel and only variants of potential or known clinical relevance were reported, as described previously.[5] The classification standards only categorize somatic variants as likely pathogenic or pathogenic based on their potential to confer growth and survival advantages in tumor cells.[8] All variants were validated through orthogonal testing using Sanger sequencing or repeat testing using next-generation sequencing. The somatic status of variants was established by sequencing remission samples, mesenchymal stromal cells[5] or inferred by a rise in variant allele frequency (VAF) in samples at progression. SNVs and indels with VAF ≥5%[3] were assessed for their association with outcome. Gene fusions were detected and filtered as previously described.[5] Candidate Ph-associated rearrangements were supported by at least 5 unique chimeric reads. Unique fusions supported by fewer chimeric reads were considered valid if they were additionally supported by evidence of corresponding genomic breaks and/or reciprocal fusions or alternative transcripts. The reliability of this strategy for the classification of high confidence somatic fusions was validated by testing diagnosis, remission or mesenchymal stromal cells using PCR and Sanger sequencing or by

repeat analysis using next-generation sequencing.[3, 5] Patients where a SNV or indel of VAF <5% was the only cancer gene variant identified, were not classed as having a clinically relevant variant. Aberrant splicing was investigated through customized pipelines and sashimi plots. All variants were reviewed using the Integrative Genomics Viewer.[3, 9]

We have previously demonstrated that RNA-based capture sequencing improved the diagnostic yield of mutant detection in CML and was capable of detecting a range of variant types.[3] These include gene fusions, RNA splice alterations and focal gene deletions in specifically targeted genes. Furthermore, intronic *BCR*::*ABL1* genomic breakpoints are detectable from pre-spliced RNA. Targeting intronic cryptic *RAG*-mediated recombination signal sequences in specific genes aids the detection of *RAG*-mediated deletions, which are common in lymphoid BP.[10] These deletions are also detectable through the generation of atypical RNA splicing.[3] Furthermore, deletions adjacent to *BCR* and/or *ABL1* can be inferred based on the presence of novel fusions involving these genes, including an estimation of the deletion size (Supplemental Table 2). Copy gain detection using this RNA-based methodology is not possible. DNA-based sequencing with the appropriate bioinformatic tools can detect copy changes but is unable to detect fusion transcripts or assess the effect of splice site variants on RNA splicing.

Supplemental Results

Complexity of Ph-associated rearrangements

Most Ph-associated rearrangements involved *BCR* and/or *ABL1* and a novel fusion partner, Figure 1. However, a small number of rearrangements involved other genes on chromosomes 9 or 22, with many of the rearrangements predicted to occur on the derivative chromosome 9. Genes such as *EXOSC2*, directly upstream of *ABL1* on chromosome 9, or the intergenic region between *EXOSC2* and *ABL1* were recurrently involved in Ph-associated rearrangements. Other recurrent fusion partner genes were *USP20* and *HMCN2*, also on chromosome 9 and upstream of *ABL1*. Interestingly, *HMCN2* is not normally expressed in blood[11] but was expressed when fused to another gene in a Ph-associated rearrangement. This highlights the potential for novel fusions to alter function.

Additional layers of genomic complexity of the Ph-associated rearrangements were sequence inversions (Supplemental Figure 1A) and/or fusions involving additional chromosomes. The Ph-associated rearrangements were a combination of genomic events and transcripts (Supplemental Figure 1B-C). When multiple Ph-associated rearrangements were identified for an individual patient, they were all linked to the primary Ph chromosome. The simplest example to illustrate Ph-associated rearrangements is shown in Supplemental Figure 5, where patient 439 had a t(9;22;12) variant Ph chromosome. Targeted RNA sequencing characterized the precise genomic breakpoints at nucleotide level resolution on each chromosome, which occurred within the *ARID2* gene on chromosome 12 and generated novel gene fusions. The *ARID2::BCR* and *ABL1::ARID2* fusion transcripts were reciprocal products of the three-way chromosomal translocation. This patient also had a 17Kb genomic inversion within *BCR* intron 14, upstream of the *BCR::ABL1* genomic break. Targeting exons of *BCR* and *ABL1* in the capture panel, plus the common intronic breakpoint regions of *BCR* was sufficient to identify the novel *ARID2* partner gene, even though this gene was not specifically targeted by probes. This case highlights how next-generation sequencing can reveal further complexity of a rearrangement. Additional chromosome involvement was also identified such as observed in patient 434 who had a variant translocation, t(9;22;19). RNA sequencing and the detection of novel gene fusions involving *BCR* and *ABL1* revealed the additional involvement of chromosome 17, as detailed in Supplemental Table 2. Overall, 11 patients had a variant Ph chromosome reported and novel fusions involving genes/sequences on the involved chromosomes were identified in 7 of these. One additional patient expressed a fusion between *ABL1* and a gene on chromosome 20 but a variant translocation was not reported.

Almost half of the Ph-associated rearrangements involved sequence inversions (Supplemental Figure 1A). These included inversions within the *BCR* gene adjacent to the *BCR*::*ABL1* genomic breakpoints (Supplemental Figure 5) and even *BCR*::*ABL1* fusions where segments of either *BCR* or *ABL1* were inverted. Moreover, some Ph-associated rearrangements may have involved the formation of possible circular DNA (Supplemental Figure 6). We did not observe a worse outcome for patients with a greater complexity of Ph-associated rearrangement.

Two patients had rearrangements involving genes upstream of *ABL1*. One was a rearrangement between *DOLK* and its adjacent gene *NUP188* that was identified using whole transcriptome sequencing and RNA panel sequencing. These genes lie approximately 2 Mb upstream of *ABL1* on chromosome 9. Cryptic deletion of *NUP188* has been reported in acute lymphoblastic leukemia.[12] However, PCR and Sanger sequencing of the diagnosis, remission and mesenchymal stromal cell samples confirmed the rearrangement was a rare germline variant and was not associated with the formation of the Ph chromosome. The second rearrangement was an inversion between *EXOSC2*, which is immediately upstream of *ABL1*, and the *FUBP3* gene approximately 70 Kb upstream of *EXOSC2*. In this case, the inversion was confirmed as somatic and likely a Ph-associated rearrangement.

Cryptic splicing of *BCR::ABL1*

Aberrant low level transcription of *BCR*::*ABL1* was evident in most patients. This frequently involved fusion between *BCR* exon 14 and *ABL1* intron 1 sequence at cryptic splice acceptor sites. Additionally, recurrent fusions between sequences within *BCR* intron 14 and *ABL1* intron 1 were frequently observed. The *BCR* fusion junctions occurred in the region between 22:23633075 and 22:23634757 (hg19 genome build) and the most frequent junction site was at 22:23633094. The fusion junctions within *ABL1* occurred over a wide region: 9:133591769 to 9:133729453. There was no association between the detection of these *BCR*::*ABL1* transcripts and outcome. The high coverage achieved with an RNA-based targeted sequencing strategy using total RNA leads to the ubiquitous detection of rare transcripts. The deep complexity of the transcriptome and the detection of rare transcripts was previously reported using a similar high depth sequencing strategy.[13] In that study, low level non-coding transcription was reported in intergenic regions and novel isoforms of well studied genes, such as *TP53*. Novel splice junctions occurred at regions that were enriched for canonical splice motifs, which is consistent with our observations involving *BCR*::*ABL1*.

Supplemental Tables (see excel file)

Supplemental Table 1: Captured genes with additional captured intronic regions

Genes included to detect fusion transcripts are indicated, including Ph-associated rearrangements on chromosomes 9 and 22. Genes included to detect RAG-mediated deletions or to aid their detection are indicated (Deletion). Some genes are mutated by various mechanisms (including fusions, deletions and indels), such as *IKZF1*, *PAX5* and *RUNX1*

Supplemental Table 2: All additional genetic abnormalities (AGAs) identified in sequenced patients

Supplemental Table 3: Evaluation of cancer gene variants and Ph-associated rearrangements for each 4-year outcome

Supplemental Table 4: Breakdown of cause of nilotinib switch, other than imatinib intolerance, based on presence of AGAs

Supplemental Figures

Supplemental Figure 1: Circos plots depicting the various Ph-associated rearrangements observed in the TIDEL-II cohort

Ph-associated rearrangements illustrated in more detail, specifically indicating the number of inversion-based events, genomic rearrangements and fusion transcripts. Some patients had multiple rearrangements. *BCR* has been divided by location for more detailed analysis. (A) Inversion based Ph-associated rearrangements are shown by turquoise ribbons linking the relevant genes; (B) Genomic Ph-associated rearrangements, identified by intronic breakpoints, are represented by red ribbons; and (C) Fusion transcripts generated by Ph-associated rearrangements are drawn in green ribbons.

Supplemental Figure 1

A. Ph-associated rearrangements involving inversions

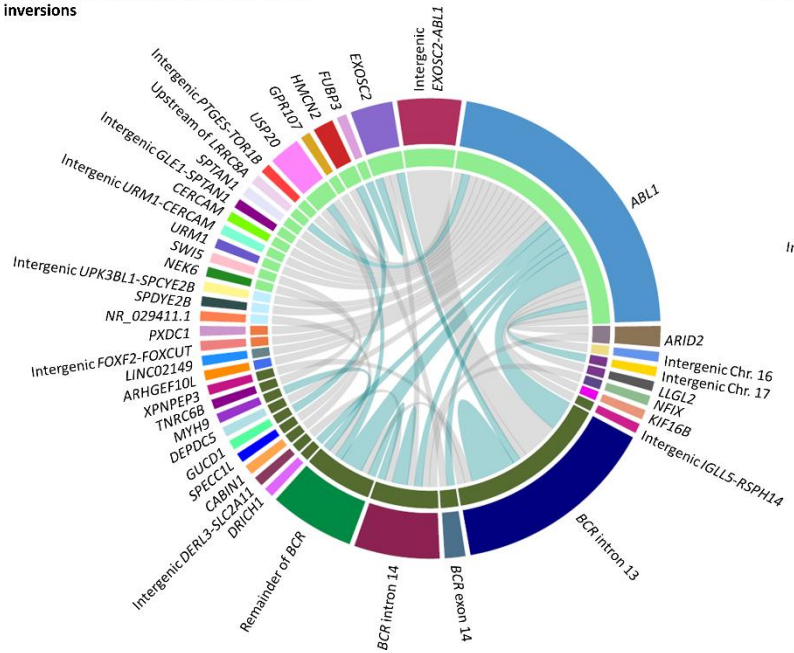

B. Genomic Ph-associated rearrangements

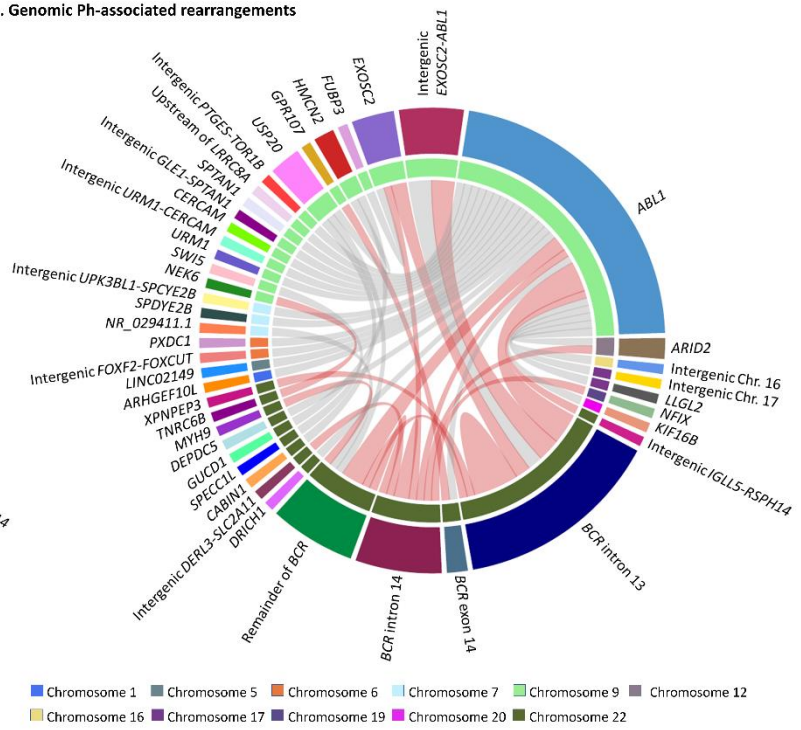

C. Ph-associated rearrangements which generated transcripts

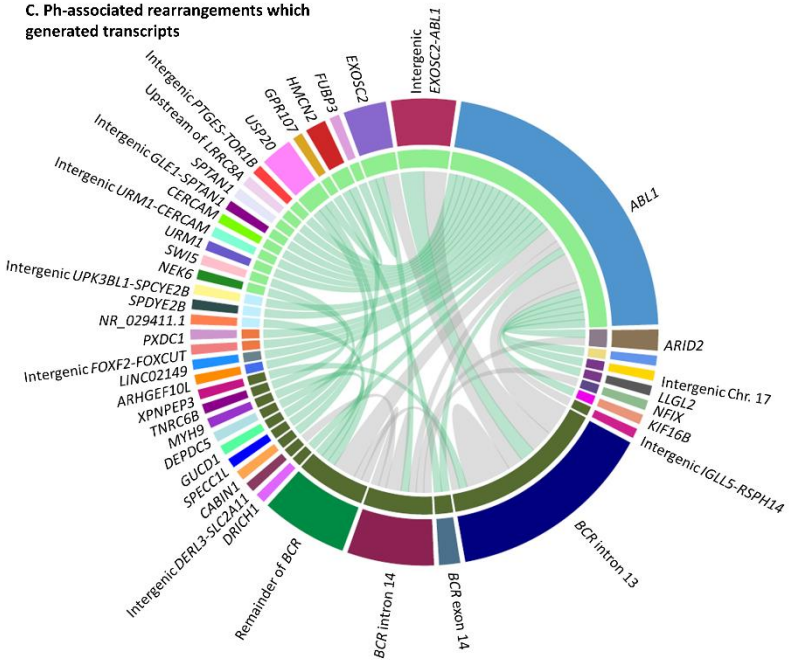

Supplemental Figure 2: Aberrant splicing observed in TIDEL-II patients

(A) One of the added benefits of utilizing RNA as the genetic material for sequencing is the ability to identify aberrant splicing. Aberrant splicing associated with a *TET2* splice acceptor variant demonstrated by an Integrative Genomics Viewer screenshot showing the wild-type sequence (top panel) and mutant (bottom panel) detectable using targeted gene panel sequencing. The mutant, detected in patient 395, disrupted the canonical splice acceptor site (AG at the exon 8 junction) and led to activation of a cryptic acceptor splice site within intron 7 (AG at the sequence read junction) and exon extension. The activated cryptic splice acceptor site was 48 nucleotides upstream of the border of exon 8. Inclusion of this sequence within the extended exon was predicted to result in premature termination. Alamut, an in-silico splice prediction tool, predicted loss of the original splice acceptor site but not activation of the cryptic splice site. (B) Sashimi plots demonstrated the atypical splicing of *TET2* between exons 7 and 8 due to the splice acceptor variant. The arcs represent splice junctions that connect exons and the number of splice junction reads are indicated. Normal splicing between exons 7 and 8 is demonstrated in the top panel. The bottom panel demonstrates normal splicing plus aberrant splicing resulting from activation of the cryptic splice site (red asterisk) within intron 7. This example demonstrates the relevance of RNA sequencing for identifying and investigating the effect of splicing variants. This somatic variant existed before the acquisition of the *BCR::ABL1* fusion.

Supplemental Figure 2

A. *TET2* splice acceptor variant NM_001127208.2:c.3955-2A>C

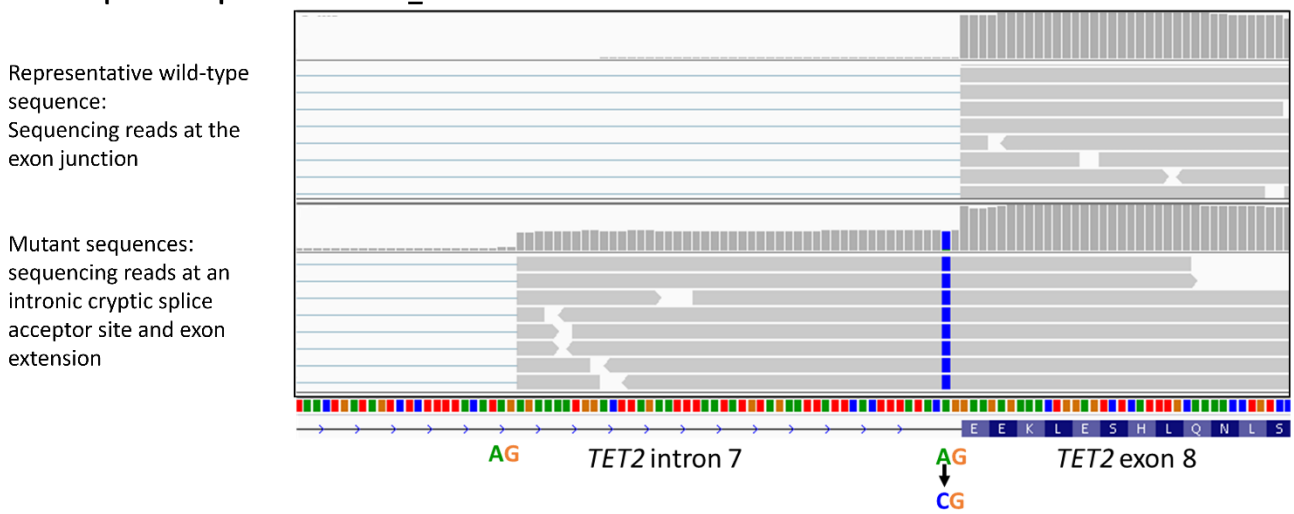

B. Aberrant RNA splicing associated with the splice acceptor variant

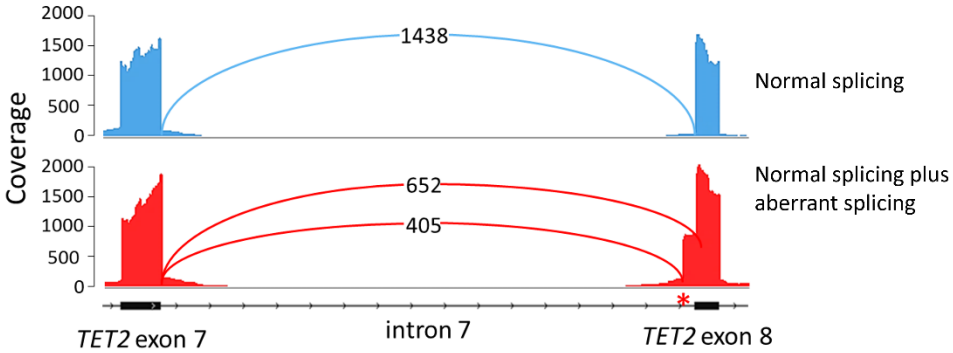

Supplemental Figure 3: Outcome and molecular responses for the study population.
No patient progressed to accelerated phase. 95% confidence intervals are indicated in grey.

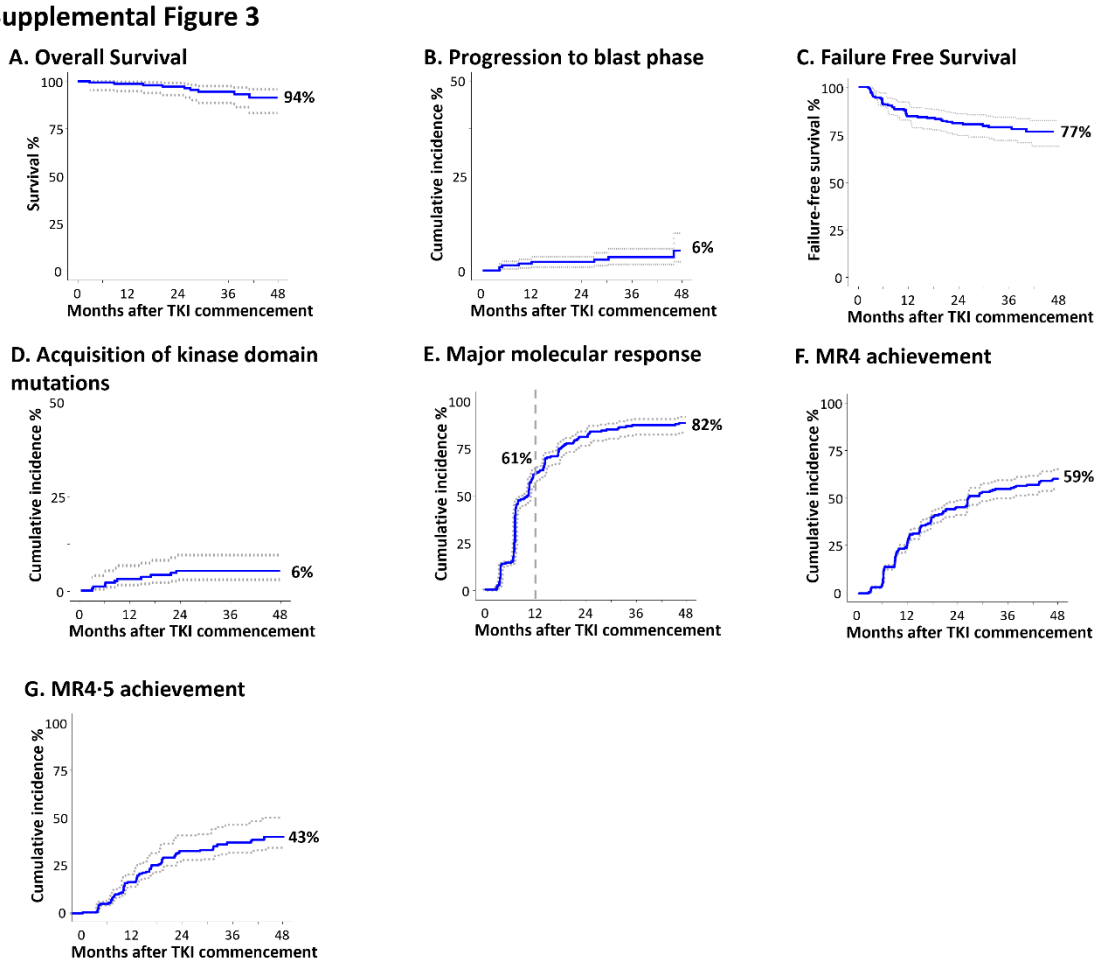

Supplemental Figure 4: Outcomes and molecular response according to the ELTS risk score

(A) Kaplan-Meier estimates of failure-free survival; (B) Cumulative incidence of MMR; (C) Cumulative incidence of MR4; (D) Cumulative incidence of MR4.5.

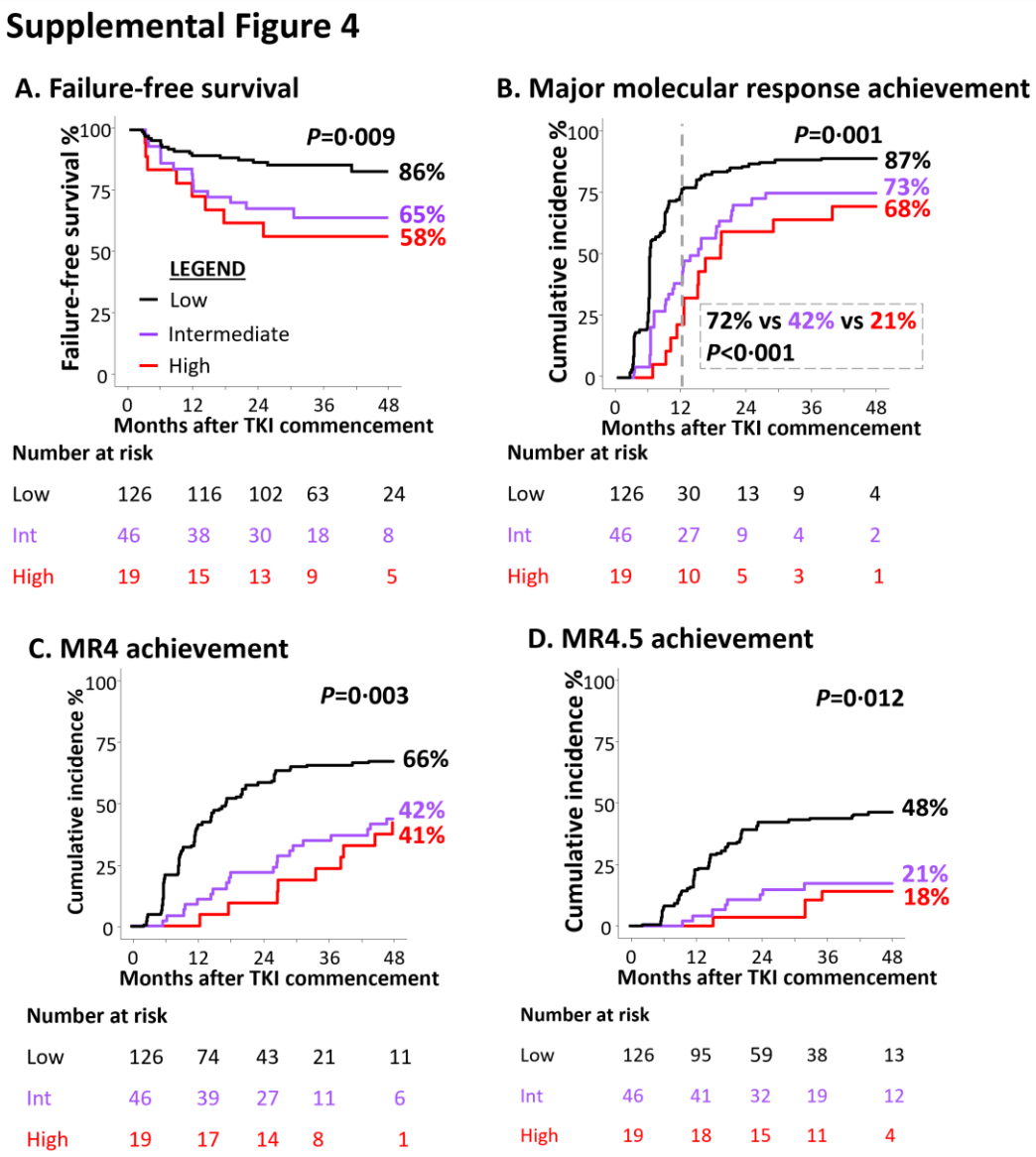

Supplemental Figure 5: Ph-associated rearrangement involving a three-way balanced translocation between chromosomes 9, 12 and 22

Patient 439 had a variant translocation involving chromosomes 9 (green), 12 (purple) and 22 (olive). The RNA-based gene panel sequencing resolved the precise genomic breakpoints and the associated gene fusions. Involvement of chromosome 12 was identified through karyotyping but RNA sequencing localized the genomic breakpoints to the *ARID2* gene at nucleotide resolution. The *ARID2::BCR* and *ABL1::ARID2* fusion transcripts were reciprocal products of the three-way chromosomal translocation. This patient also had a 17Kb genomic inversion (blue reads) within *BCR* intron 14, upstream of the *BCR::ABL1* genomic break, which was only evident using NGS. The multicolored region of each sequence read indicates that the read spans the fusion junction and that region maps to a different location in the genome. The chromosome of origin is indicated by the solid color.

Supplemental Figure 5

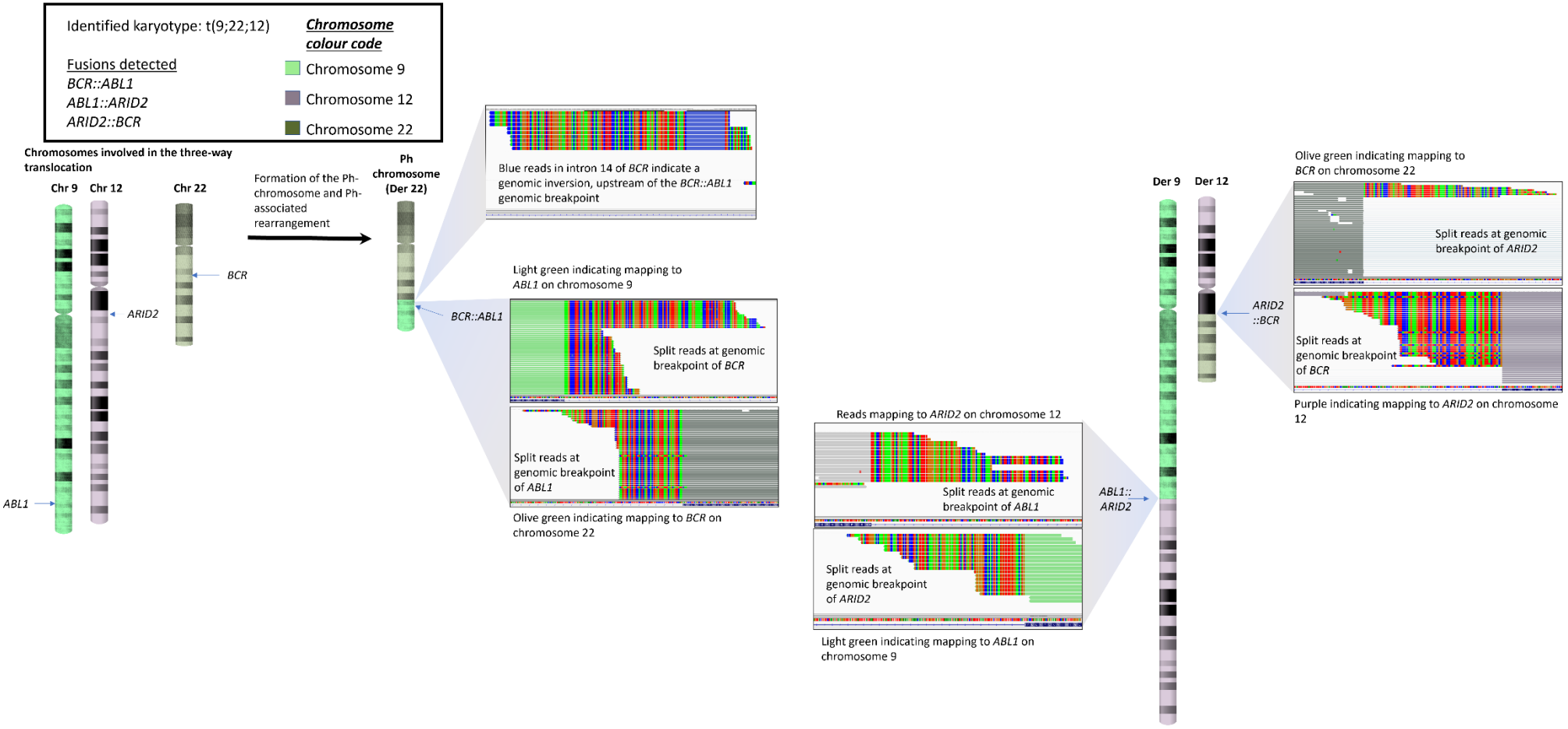

Supplemental Figure 6: Ph-associated rearrangement associated with formation of possible circularized DNA in patient 450

The orientation of the genes associated with the *XPNPEP3::BCR* e7e14 gene fusion transcript in this case suggests that a 17.7 Mb deleted sequence adjacent to the *BCR::ABL1* genomic breakpoint that extended to the *XPNPEP3* gene (downstream on chromosome 22), had possibly circularized. The *XPNPEP3::BCR* genomic breakpoints were resolved at nucleotide resolution and a corresponding *XPNPEP3::BCR* fusion transcript was detected that was likely generated by transcription of linear RNA from the circularized DNA. A corresponding *ABL1::XPNPEP3* genomic fusion may have occurred on the derivative 9 chromosome but would not be detectable if the breakpoints occurred in regions not targeted by probes. i13 indicates *BCR* intron 13 and i7 indicates *XPNPEP3* intron 7. e=exons.

Supplemental Figure 6

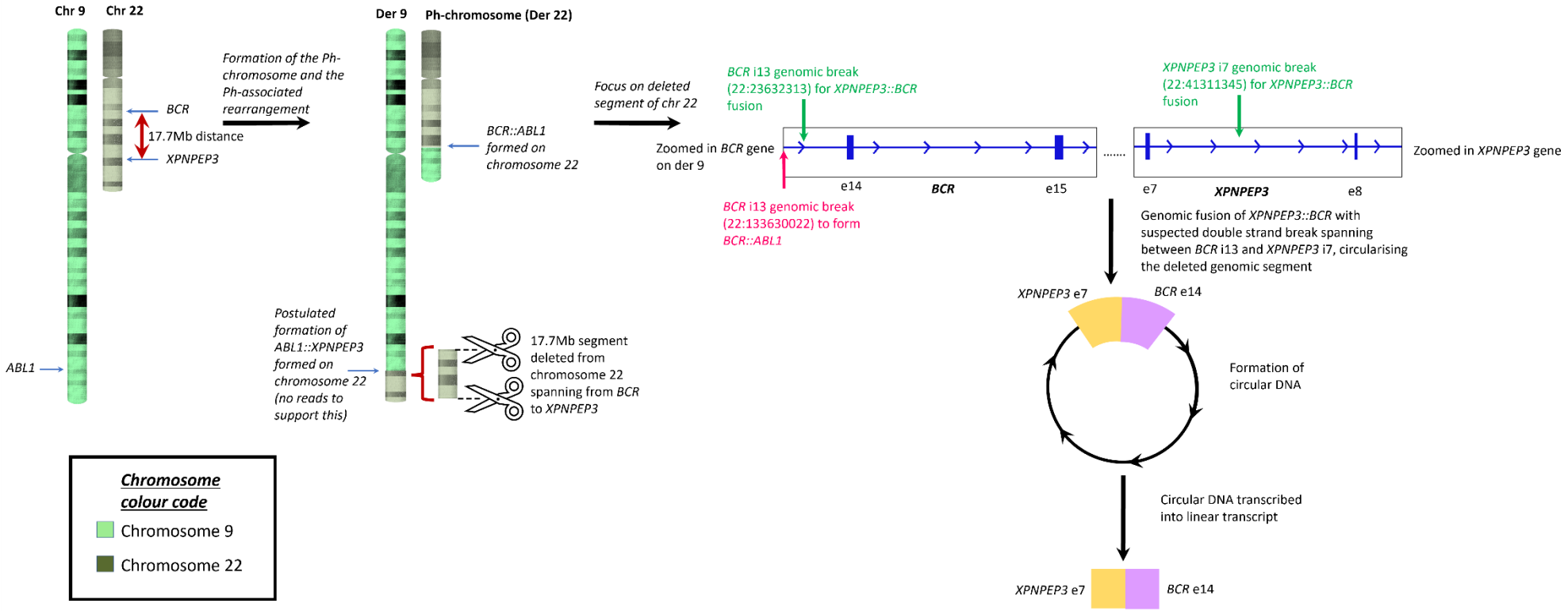

References

1. Branford S, Kim DDH, Apperley JF, Eide CA, Mustjoki S, Ong ST *et al*: Laying the foundation for genomically-based risk assessment in chronic myeloid leukemia. *Leukemia* 2019, 33(8):1835-1850.
2. Dobin A, Davis CA, Schlesinger F, Drenkow J, Zaleski C, Jha S *et al*: STAR: ultrafast universal RNA-seq aligner. *Bioinformatics* 2012, 29(1):15-21.
3. Shanmuganathan N, Wadham C, Thomson D, Shahrin NH, Vignaud C, Chaturvedi S *et al*: RNA-based targeted gene sequencing improves the diagnostic yield of mutant detection in chronic myeloid leukemia. *The Journal of molecular diagnostics : JMD* 2022, 24(7):802–822.
4. Yi K, Ju YS: Patterns and mechanisms of structural variations in human cancer. *Experimental & Molecular Medicine* 2018, 50(8):1-11.
5. Branford S, Wang P, Yeung DT, Thomson D, Purins A, Wadham C *et al*: Integrative genomic analysis reveals cancer-associated mutations at diagnosis of CML in patients with high-risk disease. *Blood* 2018, 132(9):948-961.
6. Lai Z, Markovets A, Ahdesmaki M, Chapman B, Hofmann O, McEwen R *et al*: VarDict: a novel and versatile variant caller for next-generation sequencing in cancer research. *Nucleic Acids Research* 2016, 44(11):e108-e108.
7. Benjamin D, Sato T, Cibulskis K, Getz G, Stewart C, Lichtenstein L: Calling Somatic SNVs and Indels with Mutect2. *bioRxiv* 2019:861054.
8. Horak P, Griffith M, Danos AM, Pitel BA, Madhavan S, Liu X *et al*: Standards for the classification of pathogenicity of somatic variants in cancer (oncogenicity): Joint recommendations of Clinical Genome Resource (ClinGen), Cancer Genomics Consortium (CGC), and Variant Interpretation for Cancer Consortium (VICC). *Genetics in medicine : official journal of the American College of Medical Genetics* 2022, 24(5):986-998.
9. Robinson JT, Thorvaldsdóttir H, Winckler W, Guttman M, Lander ES, Getz G *et al*: Integrative genomics viewer. *Nat Biotechnol* 2011, 29(1):24-26.
10. Thomson DW, Shahrin NH, Wang PPS, Wadham C, Shanmuganathan N, Scott HS *et al*: Aberrant RAG-mediated recombination contributes to multiple structural rearrangements in lymphoid blast crisis of chronic myeloid leukemia. *Leukemia* 2020, 34(8):2051–2063.
11. The Genotype-Tissue Expression (GTEx) project. *Nature genetics* 2013, 45(6):580-585.
12. Nowak NJ, Sait SN, Zeidan A, Deeb G, Gaile D, Liu S *et al*: Recurrent deletion of 9q34 in adult normal karyotype precursor B-cell acute lymphoblastic leukemia. *Cancer Genet Cytogenet* 2010, 199(1):15-20.
13. Mercer TR, Gerhardt DJ, Dinger ME, Crawford J, Trapnell C, Jeddeloh JA *et al*: Targeted RNA sequencing reveals the deep complexity of the human transcriptome. *Nat Biotechnol* 2011, 30(1):99-104.